# Evidence for Three-Nucleon Interaction in Isotope Shifts of $Z =$ magic Nuclei

### H. Nakada

Department of Physics, Graduate School of Science, Chiba University,
Yayoi-cho 1-33, Inage, Chiba 263-8522, Japan

**Abstract.** Density-dependence in the LS channel of the nucleonic interaction, which originates from the three-nucleon interaction, has been pointed out to account for the missing part of the $\ell s$ splitting. By incorporating the density-dependent LS channel to the semi-realistic interaction, I show that the kink in the isotope shifts of the Pb nuclei can be described fairly well within the self-consistent Hartree-Fock-Bogolyubov framework. Moreover, the almost equal charge radii between $^{40}$Ca and $^{48}$Ca are obtained by the same interaction, which has been difficult to be reproduced by such self-consistent calculations so far. The isotope shifts of the Sn nuclei are also in good agreement with the known data, and a kink is newly predicted at $N = 82$. These results are qualitatively consistent with the density-dependence of the LS channel derived from the three-nucleon force.

## 1   Introduction

As established long ago, the shell structure is fundamental to nuclear structure physics. Since nuclei are self-bound systems, the mean field (MF) is essential to the nuclear shell structure. The nuclear MF consists of a central potential that has no spin dependence, and of an $\ell s$ potential that is spin-dependent. The latter is responsible for the $\ell s$ splitting, and accounts for magic numbers greater than 20. However, it has been a long-standing problem what produces the $\ell s$ potential so strong as to give the observed size of the $\ell s$ splitting. Although the LS channels in the two-nucleon ($2N$) interaction produces a certain $\ell s$ potential, the LS channels in the bare $2N$ interaction can account for only half of the observed $\ell s$ splitting.

The nuclear shell structure is desirable to be investigated by the self-consistent MF or energy-density-functional (EDF) approaches; *i.e.*, the Hartree-Fock (HF) and Hartree-Fock-Bogolyubov (HFB) approaches. With respect to the missing part of the $\ell s$ potential, there were a lot of arguments; *e.g.*, a second-order effect of the tensor force and a relativistic effect. Although the tensor force indeed has sizable contribution like the LS force in its second order [1], the tensor-force effect was found to be insufficient to reproduce the observed $\ell s$ splitting [2]. In the relativistic mean-field (RMF) approaches, the $\ell s$ potential is additively

contributed by the scalar potential and the time-component of the vector potential [3]. Despite certain attraction in this picture, the size of the scalar and vector potentials has been parametrized and has not been connected well to the bare nucleonic interaction.

It has recently been pointed out that the $3N$ interaction derived by the chiral effective field theory ($\chi$EFT) significantly contributes to the $\ell s$ potential [4]. The $3N$ interaction effectively adds a density-dependence to the LS channel, which enhances the LS interaction as the density grows. In order to confirm this picture, it is desired to apply it to other physical quantities that are independent of the $\ell s$ splitting itself. For this purpose, it is recalled that the kink in the isotope shifts of the Pb nuclei [5] seems to correlate to the LS interaction. It could provide us with a unique opportunity to investigate property of the LS interaction in nuclei, not necessarily correlating to the $\ell s$ splitting.

The author has developed the so-called *semi-realistic* effective interaction [6, 7], which is based on the M3Y interaction [8, 9] that was derived from the $G$-matrix, and have applied it to the self-consistent MF and RPA calculations. Since it has yet been difficult, despite significant progress, to describe all the basic nuclear properties in fully microscopic manners from the bare nucleonic interaction, several parameters have been modified so as to reproduce basic nuclear properties, *e.g.*, the saturation properties. The parameter-set M3Y-P6 [7] and its variant M3Y-P6a [10] will be mainly used in this paper. In the former the $2N$ LS interaction is enhanced so as to reproduce the $\ell s$ splitting within the MF regime, by which we have investigated the shell structure from stable to unstable nuclei. It should be mentioned that the tensor channels in this interaction is realistic, not changed from that of the original $G$-matrix-based M3Y-Paris interaction [9]. On the other hand, a density-dependent LS channel is added in M3Y-P6a, instead of enhancing the $2N$ LS channel, while all the other channels in M3Y-P6 are maintained. We have applied these interactions to the isotope shifts of the $Z = $ magic nuclei within the self-consistent MF regime. Comparison between M3Y-P6 and P6a will address effects of the $3N$ LS interaction clearly.

## 2   M3Y-Type Interaction and Mean-Field Calculations

We use the non-relativistic nuclear Hamiltonian,

$$H_N = K + V_N\,; \quad K = \sum_i \frac{\mathbf{p}_i^2}{2M}\,, \quad V_N = \sum_{i<j} v_{ij}\,, \tag{1}$$

where $i$ and $j$ are the indices of individual nucleons. The effective interaction $v_{ij}$ is comprised of the following channels,

$$v_{ij} = v_{ij}^{(\mathrm{C})} + v_{ij}^{(\mathrm{LS})} + v_{ij}^{(\mathrm{TN})} + v_{ij}^{(\mathrm{C}\rho)} + v_{ij}^{(\mathrm{LS}\rho)}\,, \tag{2}$$

215

where

$$v_{ij}^{(C)} = \sum_n \left( t_n^{(SE)} P_{SE} + t_n^{(TE)} P_{TE} + t_n^{(SO)} P_{SO} + t_n^{(TO)} P_{TO} \right) f_n^{(C)}(r_{ij}) ,$$

$$v_{ij}^{(LS)} = \sum_n \left( t_n^{(LSE)} P_{TE} + t_n^{(LSO)} P_{TO} \right) f_n^{(LS)}(r_{ij}) [\mathbf{L}_{ij} \cdot (\mathbf{s}_i + \mathbf{s}_j)] ,$$

$$v_{ij}^{(TN)} = \sum_n \left( t_n^{(TNE)} P_{TE} + t_n^{(TNO)} P_{TO} \right) f_n^{(TN)}(r_{ij}) \, r_{ij}^2 S_{ij} , \qquad (3)$$

$$v_{ij}^{(C\rho)} = \left( C^{(SE)}[\rho(\mathbf{r}_i)] P_{SE} + C^{(TE)}[\rho(\mathbf{r}_i)] P_{TE} \right) \delta(\mathbf{r}_{ij}) ,$$

$$v_{ij}^{(LS\rho)} = 2i \, D[\rho(\mathbf{R}_{ij})] \, \mathbf{p}_{ij} \times \delta(\mathbf{r}_{ij}) \, \mathbf{p}_{ij} \cdot (\mathbf{s}_i + \mathbf{s}_j) .$$

In the above equations, $\mathbf{r}_{ij} = \mathbf{r}_i - \mathbf{r}_j$, $\mathbf{p}_{ij} = (\mathbf{p}_i - \mathbf{p}_j)/2$, $\mathbf{L}_{ij} = \mathbf{r}_{ij} \times \mathbf{p}_{ij}$, $\mathbf{R}_{ij} = (\mathbf{r}_i + \mathbf{r}_j)/2$, $\mathbf{s}$ is the spin operator, $S_{ij} = 4 \left[ 3(\mathbf{s}_i \cdot \hat{\mathbf{r}}_{ij})(\mathbf{s}_j \cdot \hat{\mathbf{r}}_{ij}) - \mathbf{s}_i \cdot \mathbf{s}_j \right]$, and $\rho(\mathbf{r})$ denotes the nucleon density. $P_Y$ represents the projection operator on the two-particle channel Y (Y = SE, TE, SO, TO). In the M3Y-type interactions, we take $f_n^{(X)}(r) = e^{-\mu_n^{(X)} r} / \mu_n^{(X)} r$ for all the density-independent channels X = C, LS, TN.

It is reasonable to assume the density-dependent channels $v^{(C\rho)}$ and $v^{(LS\rho)}$ to have a short-range character. $v^{(C\rho)}$ may originate from the $3N$ interaction as well as from the density-dependence addressed by the medium effects, and is quite relevant to the saturation properties. For the density-dependent coupling, we adopt the form $C^{(Y)}[\rho] = t_\rho^{(Y)} \rho^{\alpha^{(Y)}}$. Until recently, only $v^{(LS)}$ (i.e., density-independent $2N$ force) had been considered for the LS channel. For instance, $v^{(LS\rho)}$ is not taken into account in M3Y-P6 and $v^{(LS)}$ of the M3Y-Paris interaction is enhanced by about twice. In contrast, $v^{(LS\rho)}$ has been taken into account in M3Y-P6a, so that it should qualitatively be consistent with the $\chi$EFT indication, by taking the density-dependence as

$$D[\rho(\mathbf{r})] = -w_1 \frac{\rho(\mathbf{r})}{1 + d_1 \rho(\mathbf{r})} . \qquad (4)$$

The parameter $d_1$ is fixed to be $1.0\,\mathrm{fm}^3$, which has been used to suppress instability at extremely high densities. In order to separate out effects independent of the $\ell s$ splitting, we have fixed $w_1$ in M3Y-P6a by fitting to the M3Y-P6 result of $n0i_{13/2}$-$n0i_{11/2}$ splitting at $^{208}$Pb.

The full Hamiltonian is $H = H_N + V_C - H_{\mathrm{c.m.}}$; $V_C$ and $H_{\mathrm{c.m.}}$ ($= \mathbf{P}^2 / 2AM$) are the Coulomb interaction and the center-of-mass (c.m.) Hamiltonian, respectively. The results using M3Y-P6 represents those using interactions without $\rho$-dependence in the LS channel. In order to confirm this point, we also use the Gogny-D1M interaction [13] for $V_N$. For numerical calculations, the Gaussian expansion method is applied [11], whose basis functions are detailed in Ref. [12].

## 3 Shell Structure Reproduced by M3Y-P6

For the isotope shifts of the Pb nuclei, the kink at $N = 126$ was experimentally established, as mentioned earlier. In the theoretical studies in '90s [14], the slightly larger radius of $n0i_{11/2}$ than the surrounding orbits was suggested to be responsible for the kink. The radius of $n0i_{11/2}$ can contribute to the isotope shifts in $N > 126$ if sizable excitation out of $n1g_{9/2}$ to $n0i_{11/2}$ is contained in the ground states of the Pb nuclei. Therefore, the shell structure, the energy difference between $n1g_{9/2}$ and $n0i_{11/2}$ to be specific, is quite relevant to this problem.

It is surveyed here that the M3Y-type semi-realistic interactions, M3Y-P6 in particular, is successful in describing the nuclear shell structure from stable to unstable nuclei. It has been pointed out [15] that the tensor force $v^{(\mathrm{TN})}$ is important in the $Z$- or $N$-dependence of the shell structure. One of such examples is seen in the s.p. energy difference between $p0d_{3/2}$ and $p1s_{1/2}$ in the Ca nuclei. In general, it is difficult to compare the s.p. levels in the HF approach with experiments even for doubly magic nuclei, because of their fragmentation. If the spectroscopic factors of the relevant levels are sufficiently measured, the s.p. energies near the doubly-closed core are extracted experimentally via the average weighted by the spectroscopic factors, which can be compared to the HF results. An interesting case is obtained in vicinity of $^{40}$Ca and $^{48}$Ca, where the spectroscopic factors of $p0d_{3/2}^{-1}$ and $p1s_{1/2}^{-1}$ levels have been measured exhaustively [16, 17]. The experimental results indicate an inversion of the two levels when going from $^{40}$Ca to $^{48}$Ca. It has been found that the slope of the s.p. energy difference from $^{40}$Ca to $^{48}$Ca is nicely reproduced by the M3Y-type interaction that contains the realistic tensor force [18], including M3Y-P6 [19]. While a similar result is obtained in the relativistic HF calculation with the tensor force [20], this is difficult if we use interactions without including the tensor force explicitly [21].

In Ref. [22], magic numbers have been investigated in a wide range of the nuclear chart, including light to heavy and stable to unstable nuclei, within the self-consistent MF framework. It should be stated how the magic numbers were identified. Magic $Z$ or $N$ takes place when the shell gap is large and thereby many-body correlations are strongly quenched. For instance, the spherical HF solution should be a good approximation of the ground state in doubly magic nuclei. The shell gap is well evaluated within the spherical HF framework. In order to compare the shell gap to the strength of the many-body correlations, we use the pairing correlation as a measure, because it is usually dominant near the magicity. Implementing the spherical HFB calculations, we have identified $Z$ ($N$) to be magic when the proton (neutron) pair correlation vanishes in the HFB solution. This identification is useful to search candidates of magic numbers, up to their $Z$- and $N$-dependence. We have also picked up submagic numbers if the condensate energy $E_{\mathrm{HF}} - E_{\mathrm{HFB}}$ is smaller than a certain critical value, for which we have taken $0.5\,\mathrm{MeV}$ and $0.8\,\mathrm{MeV}$. It is then found that the M3Y-

P6 interaction gives good prediction of magic numbers, without contradiction against available experimental data apart from a few exceptions. Notable examples are seen in submagic nature of $N = 16$ at $^{24}$O, $N = 32$ at $^{52}$Ca, $N = 40$ at $^{68}$Ni, $Z = 64$ at $^{146}$Gd, and loss of the $N = 28$ magicity in $Z \leq 14$. To certain degree this success of M3Y-P6 owes to the realistic tensor force, although role of other channels should not be underestimated. Note that, when the breakdown of magicity is predicted in this study, it is not obvious what correlation is responsible for the breakdown in actual, only implying that the shell gap is not large enough to keep the magicity. There are two regions of disagreement. One is $^{32}$Mg, at which experiments have confirmed that the $N = 20$ magicity is broken. The spherical HFB study with M3Y-P6 has predicted that the magicity is kept, as with the other interactions, although the loss of the magicity at $^{30}$Ne is reproduced. This problem may be solved by taking the quadrupole deformation into consideration explicitly. The axial HF calculation gives well-deformed configuration at close energy to the nearly spherical minimum [23]. An axial HFB calculation including the angular-momentum projection is awaited. Another region of disagreement is the $N \gtrsim 60$ Zr nuclei. Although deformation has been established experimentally, the spherical HFB predicts $Z = 40$ to be magic in these nuclei. The axial HF calculation suggests again that this is likely to be resolved by the quadrupole deformation [24].

## 4 Isotope Shifts of $Z = $ magic Nuclei

The X-ray frequencies in the atomic excitation and deexcitation suffer slight shifts among isotopes, owing to the difference in the reduced mass of an electron (mass shift) and to the difference in the Coulomb field produced by the nucleus (field shift). Convertible to the difference in the nuclear charge radii, the latter is subject to nuclear structure physics. We shall hereafter consider only field shifts under the name of isotopes shifts, as is customary in nuclear structure physics, The isotope shifts often reveal structural evolution of nuclei for increasing $N$; *e.g.*, transition from spherical to deformed shape. In addition, data of the isotope shifts in some $Z = $ magic nuclei, which are usually spherical, have cast questions on the predictivity of nuclear structure theories. We have reinvestigated the isotope shifts of $Z = $ magic nuclei in the spherical HFB calculations, using M3Y-P6a which contain the $\rho$-dependent LS channel [10, 25].

Although the M3Y-P6 interaction well reproduces the shell structure, $v^{(\mathrm{LS})}$ in M3Y-P6 is not realistic, since it is phenomenologically enhanced from the LS channels of the M3Y-Paris interaction. In M3Y-P6a, we add a $\rho$-dependent LS interaction $v^{(\mathrm{LS}\rho)}$, which is inspired by the $3N$ LS interaction, instead of enhancing $v^{(\mathrm{LS})}$. The other channels of M3Y-P6a are identical to those of M3Y-P6. Most MF results are not very different between M3Y-P6 and M3Y-P6a. In particular, as the strength of $v^{(\mathrm{LS}\rho)}$ has been fitted to the $n0i_{13/2}$-$n0i_{11/2}$ splitting with M3Y-P6, the $\ell s$ splitting is similar between M3Y-P6 and M3Y-P6a. However, there is difference in the s.p. functions, which is slight but not

always negligible. Because of the $\rho$-dependence, $v^{(\mathrm{LS}\rho)}$ becomes stronger as the density increases, which makes the $\ell s$ potential stronger in the nuclear interior, and *vice versa*. As a result, the s.p. function of the $j = \ell + 1/2$ ($j = \ell - 1/2$) orbit shifts inward (outward) in the M3Y-P6a results, compared to the M3Y-P6 results, as has been confirmed in Figure 1 of Ref. [10]. This mechanism may affect the isotope shifts of the $Z = \mathrm{magic}$ nuclei; *e.g.*, Pb.

### 4.1 Pb isotopes

The isotope shifts of the Pb nuclei are usually defined by taking $^{208}$Pb as a reference, $\Delta\langle r^2\rangle_p(^A\mathrm{Pb}) := \langle r^2\rangle_p(^A\mathrm{Pb}) - \langle r^2\rangle_p(^{208}\mathrm{Pb})$. The kink has been observed at $N = 126$ [5, 26] when $\Delta\langle r^2\rangle_p(^A\mathrm{Pb})$ is plotted as a function of $N$. While this kink was unable to be reproduced with the conventional Skyrme EDF [29], a relativistic MF approach gave a kink at $N = 126$ [27] by taking account of the pairing. It turned out that the isospin content in the LS channel of the EDF makes this difference [27], leading to an extension of the Skyrme EDF [14]. However, there remains a problem.
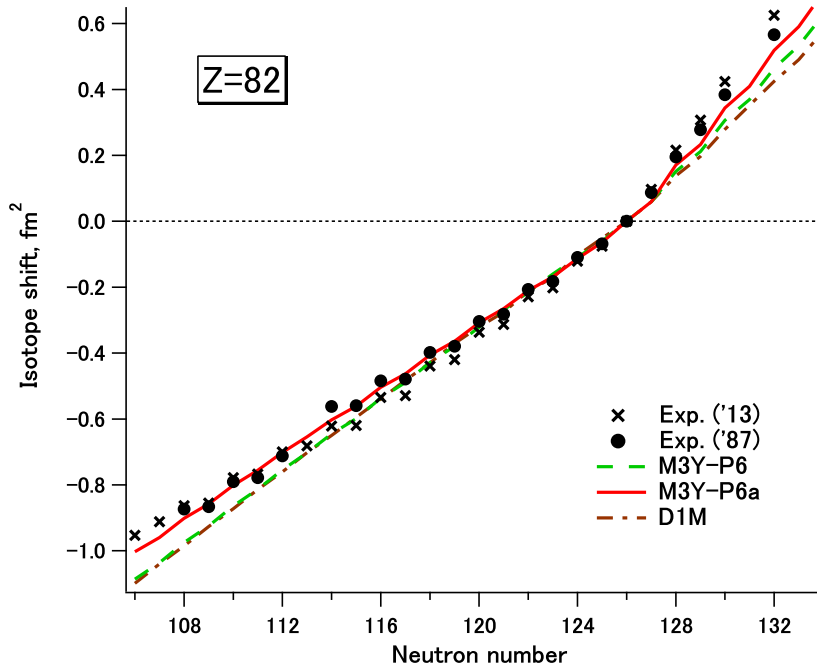


Figure 1. Isotope shifts of the Pb nuclei, $\Delta\langle r^2\rangle_p(^A\mathrm{Pb})$, obtained from the spherical HFB calculations with M3Y-P6a (red solid line), in comparison to those with M3Y-P6 (green dashed line) and D1M (blue dot-dashed line). Experimental data are quoted from Refs. [26] (crosses) and [5] (circles).

It is reasonable to consider that the lowest s.p. level above $N = 126$ is $n1g_{9/2}$, as typically indicated by the lowest level in $^{209}$Pb [28]. Although occupation on $n1g_{9/2}$ does not produce a kink [14, 29], neutrons excited to $n0i_{11/2}$ may yield a kink. Such excitation is possible because of the pair correlation. Therefore the s.p. energy spacing between $n1g_{9/2}$ and $n0i_{11/2}$ is important. In both of the RMF and the modified Skyrme EDF, the two s.p. levels $n1g_{9/2}$ and $n0i_{11/2}$ are almost degenerate within $\sim 0.1\,\mathrm{MeV}$ [14], which makes the occupation probabilities of the two levels almost equal. Otherwise the kink was too weak, not comparable to the observed one [29]. However, experimental data does not support this degeneracy. For instance, the energy difference between $9/2^+$ and $11/2^+$ state is $\sim 0.8\,\mathrm{MeV}$ at $^{209}$Pb. This problem had not been solved for two decades.

When the $\rho$-dependent LS interaction is considered, the mean radius of $n0i_{11/2}$, a $j = \ell - 1/2$ orbit, increases. If $n0i_{11/2}$ is occupied to a certain extent, the proton distribution may become broader owing to the proton-neutron attraction. To see whether this effect improves the kink problem of Pb, the HFB results with M3Y-P6a (red solid line) of $\Delta\langle r^2\rangle_p(^A\mathrm{Pb})$ are compared with those with M3Y-P6 (green dashed line) in Figure 1.

Because the $\ell s$ splitting has been adjusted, the s.p. energy difference $\varepsilon(n0i_{11/2}) - \varepsilon(n1g_{9/2})$ of M3Y-P6a is similar to that of M3Y-P6. The difference with M3Y-P6a is $0.72\,\mathrm{MeV}$ at $^{208}$Pb, close to the measured difference between $9/2^+$ and $11/2^+$ at $^{209}$Pb ($0.78\,\mathrm{MeV}$). Nevertheless, the kink in the isotope shifts at $N = 126$ is stronger than with M3Y-P6 because of the $\rho$-dependence in the LS channel. It is in fair agreement with the observed kink, comparable to the results in Refs. [14, 27]. It is noted that the moderate value of $\varepsilon(n0i_{11/2}) - \varepsilon(n1g_{9/2})$ originates from the isospin content of the M3Y interaction to a certain extent [see Eq. (3)].

One may wonder if correlations beyond the MF approximation may solve the kink problem of the isotope shifts, even with the interactions that do not contain $v^{(\mathrm{LS}\rho)}$. However, although the generator-coordinate method was applied in Ref. [30], it was found that the correlations beyond the MF approximation hardly influence the isotope shifts of the Pb nuclei around $N = 126$.

## 4.2   Ca isotopes

It has long been known that $^{40}$Ca and $^{48}$Ca have very similar charge radii. However, this experimental fact has been difficult to be accounted for by self-consistent theories. The $\rho$-dependence in the LS interaction may shed new light on this subject.

Because both of these two nuclei are doubly magic, they are expected to be well described in the spherical HF framework. The $n0f_{7/2}$ orbit becomes populated when going from $^{40}$Ca to $^{48}$Ca. Attraction from the neutrons occupying $0f_{7/2}$ mainly control difference of the charge radii. Because of the $j = \ell + 1/2$ nature, the s.p. function of $n0f_{7/2}$ tends to shrink, if the $\rho$-dependent LS interaction is used. This inhibits increase of the charge radius of $^{48}$Ca relative to that of
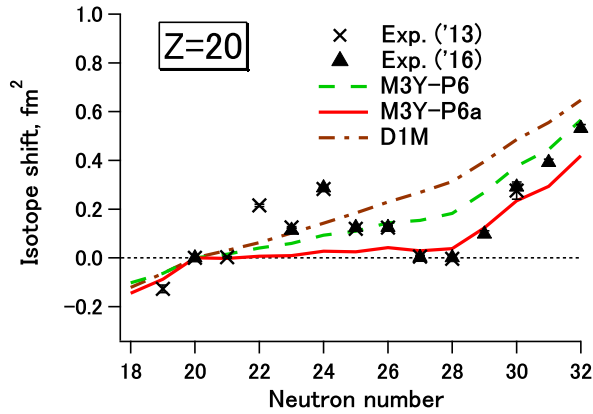
Figure 2. Isotope shifts of the Ca nuclei $\Delta\langle r^2\rangle_p(^A\mathrm{Ca})$. Experimental data are taken from Ref. [31] (triangles) as well as from [26] (crosses). See Figure 1 for other conventions. Modified from Figure 2 of Ref. [25].

$^{40}$Ca, being able to reproduce the nearly equal charge radii between them. This is exemplified in Figure 2 in terms of the isotope shifts, in which the spherical HFB results with M3Y-P6a are compared with those with M3Y-P6 as well as with the experimental data. The isotopes shifts of the Ca nuclei are defined by taking $^{40}$Ca as a reference; $\Delta\langle r^2\rangle_p(^A\mathrm{Ca}) := \langle r^2\rangle_p(^A\mathrm{Ca}) - \langle r^2\rangle_p(^{40}\mathrm{Ca})$. See Ref. [25] for detailed analysis.

It is reported [31] very recently that *ab initio* calculations with the $\chi$EFT $2N + 3N$ interaction reproduce the close radii between $^{40}$Ca and $^{48}$Ca. The present MF results with the semi-realistic interaction seem consistent with the *ab initio* results, and tell us that the $3N$ LS interaction is essential to solve this problem.

The measured isotope shifts of $^{42-46}$Ca show irregular behavior, staggering and far from monotonic. It was suggested [32] that excitations out of the $^{40}$Ca core are needed to solve this problem; an effect beyond the MF regime.

## 4.3 Sn isotopes

In the previous subsections we have shown that the long-standing problems with respect to the isotope shifts in Ca and Pb can be solved by the $3N$ or $\rho$-dependent LS interaction. It will also be of interest to give new predictions based on the $3N$ LS interaction. As such an example we next present the isotope shifts of the Sn nuclei in Figure 3, $\Delta\langle r^2\rangle_p(^A\mathrm{Sn}) := \langle r^2\rangle_p(^A\mathrm{Sn}) - \langle r^2\rangle_p(^{120}\mathrm{Sn})$.

We find that $\Delta\langle r^2\rangle_p(^A\mathrm{Sn})$ is well reproduced by the spherical HFB calculations with M3Y-P6a in a long chain of the Sn isotopes. In particular, the curve in $70 < N < 82$ is in good agreement with the data. In this region neutrons are mainly occupying the $0h_{11/2}$ orbit, whose radius is suppressed by the $\rho$-dependent LS interaction. By this mechanism, the slope of $\Delta\langle r^2\rangle_p(^A\mathrm{Sn})$ in
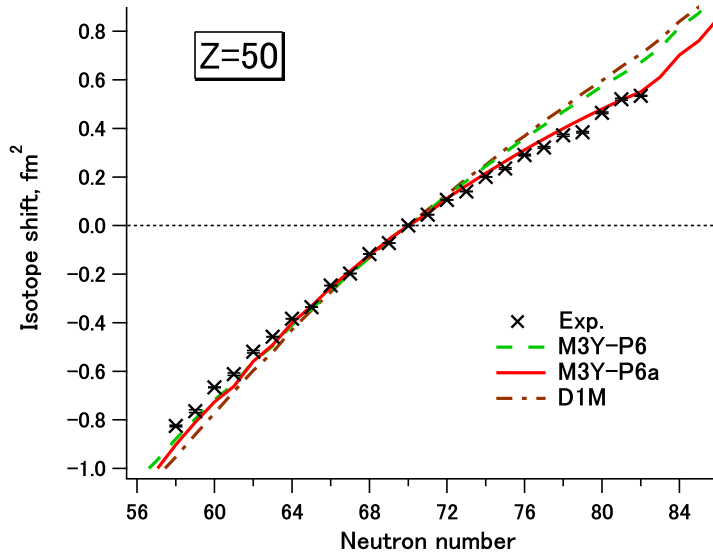
Figure 3. Isotope shifts of the Sn nuclei $\Delta\langle r^2\rangle_p(^A\mathrm{Sn})$. See Figure 1 for conventions. Modified from Figure 4 of Ref. [25].

$70 < N < 82$ is reduced in the M3Y-P6a result. It is also remarked that a kink is predicted at $N = 82$ with M3Y-P6a, unlike those with the other interactions. This kink takes place for a similar reason to the Pb case. While the lowest s.p. level beyond $N = 82$ is $n1f_{7/2}$, $n0h_{9/2}$ is partially occupied because of the pair correlation. The s.p. function of $n0h_{9/2}$ produced by M3Y-P6a is broader than that produced by M3Y-P6, and makes the slope of $\Delta\langle r^2\rangle_p(^A\mathrm{Sn})$ steeper at $N > 82$. Isotope-shift measurements in $N > 82$ will be intriguing, which may provide us with a good test of the present scheme based on the $3N$ LS interaction.

## 5 Summary

Based on the successful description of the nuclear shell structure in the MF calculations with the semi-realistic M3Y-P6 interaction, we have incorporated the $\rho$-dependent LS channel suggested by the $\chi$EFT, deriving a variant interaction M3Y-P6a. By comparing the spherical HFB results with M3Y-P6a to those with M3Y-P6, we have investigated effects of the $\rho$-dependent LS channel on the isotope shifts of $Z = \mathrm{magic}$ nuclei. The kink of the isotope shifts at $N = 126$ in the Pb nuclei is reproduced fairly well by M3Y-P6a, without fictitious degeneracy between $n1g_{9/2}$ and $n0i_{11/2}$. Almost equal charge radii between $^{40}\mathrm{Ca}$ and $^{48}\mathrm{Ca}$ are also described nicely. The isotope shifts of the Sn nuclei are reproduced in a long chain as well, and a kink is newly predicted at $N = 82$. In all of them,

the $\rho$-dependence in the LS channel plays a crucial role, and they qualitatively support the $3N$ interaction derived by the $\chi$EFT.

## Acknowledgements

## References

[1] A. Arima and T. Terasawa, *Prog. Theor. Phys.* **23** (1960) 115.

[2] K. Andō and H. Bandō, *Prog. Theor. Phys.* **66** (1981) 227.

[3] B.D. Serot and J.D. Walecka, *Adv. Nucl. Phys.* **16** (1986) 1.

[4] M. Kohno, *Phys. Rev. C* **86** (2012) 061301(R).

[5] P. Aufmuth, K. Heilig and A. Steudel, *At. Data Nucl. Data Tables* **37** (1987) 455.

[6] H. Nakada, *Phys. Rev. C* **68** (2003) 014316.

[7] H. Nakada, *Phys. Rev. C* **87** (2013) 014336.

[8] G. Bertsch *et al.*, *Nucl. Phys. A* **284** (1977) 399.

[9] N. Anantaraman, H. Toki and G.F. Bertsch, *Nucl. Phys. A* **398** (1983) 269.

[10] H. Nakada and T. Inakura, *Phys. Rev. C* **91** (2015) 021302(R).

[11] H. Nakada, *Nucl. Phys. A* **764** (2006) 117; *ibid.* **801** (2008) 169.

[12] H. Nakada, *Nucl. Phys. A* **808** (2008) 47.

[13] S. Goriely *et al.*, *Phys. Rev. Lett.* **102** (2009) 242501.

[14] P.-G. Reinhard and H. Flocard, *Nucl. Phys. A* **584** (1995) 467.

[15] T. Otsuka *et al.*, *Phys. Rev. Lett.* **95** (2005) 232502.

[16] P. Doll *et al.*, *Nucl. Phys. A* **263** (1976) 210.

[17] C.A. Ogilvie *et al.*, *Nucl. Phys. A* **465** (1987) 445.

[18] H. Nakada, K. Sugiura and J. Margueron, *Phys. Rev. C* **87** (2013) 067305.

[19] H. Nakada *et al.*, *Eur. Phys. J. A* 52 (2016) 185.

[20] J.J. Li *et al.*, *Phys. Lett. B* **753** (2015) 97.

[21] M. Grasso *et al.*, *Phys. Rev. C* **76** (2007) 044319.

[22] H. Nakada and K. Sugiura, *Prog. Theor. Exp. Phys.* (2014) 033D02.

[23] Y. Suzuki, H. Nakada and S. Miyahara, *Phys. Rev. C* **94** (2016) 024343.

[24] S. Miyahara and H. Nakada, unpublished.

[25] H. Nakada, *Phys. Rev. C* **92** (2015) 044307.

[26] I. Angeli and K.P. Marinova, *At. Data Nucl. Data Tables* **99** (2013) 69.

[27] M.M. Sharma, G. Lalazissis and P. Ring, *Phys. Lett. B* **317** (1994) 9.

[28] R.B. Firestone *et al.*(eds.), *Table of Isotopes*, $8^{th}$ ed., John Wiley & Sons, New York (1996).

[29] P.M. Goddard, P.D. Stevenson and A. Rios, *Phys. Rev. Lett.* **110** (2013) 032503.

[30] M. Bender, G.F. Bertsch and P.-H. Heenen, *Phys. Rev. C* **73** (2006) 034322.

[31] R.F. Garcia Ruiz *et al.*, *Nat. Phys.* **12** (2016) 594.

[32] E. Caurier *et al.*, *Phys. Lett. B* **522** (2001) 240.